

Proceedings of Meetings on Acoustics

Volume 16, 2012

<http://acousticalsociety.org/>

XVII International Conference on Nonlinear Elasticity in Materials
Cefalu, Sicily, Italy
1 - 7 July 2012
Session PA: Physical Acoustics

First simulations of the candy can concept for high amplitude non-contact excitation

Steven Delrue, Pierre-Yves Le Bas, T. J. Ulrich, Brian Anderson and Koen Van Den Abeele*

*Corresponding author's address: Physics, Wave Propagation and Signal Processing, KU Leuven, KULAK, Kortrijk, 8500, West-Flandres, Belgium, Koen.VanDenAbeele@kuleuven-kulak.be

Nonlinear acoustic techniques have proven to be extremely sensitive to early stage damage detection. However, the main issue preventing widespread use of these techniques is that they require high amplitude waves to induce the nonlinear response. As an alternative to transducers bonded to the test material, a more practical realization consists of developing non-contact ultrasonic transducers capable of generating high amplitude waves. Time reversal (TR) techniques are particularly suited to concentrate sound energy at a chosen location in space and at a specific instance in time. In this paper, it is numerically demonstrated how TR and a "candy can" (i.e. a highly scattering, contained medium) can be used to create a focused, high amplitude non-contact transducer. We developed and investigated the results of a finite element model of the "candy can" concept. The model allows to demonstrate the concept in different situations and illustrates the ability to pre-calibrate the non-contact source in air. The results of the simulations allow a better insight in the new concept and will be used in a further stadium for optimization of the high amplitude non-contact source.

Published by the Acoustical Society of America through the American Institute of Physics

I. INTRODUCTION

Nonlinear Elastic Wave Spectroscopy (NEWS) is one of the most sensitive techniques for detecting incipient damage in materials [1]. However, NEWS techniques require large wave amplitudes in order to trigger the nonlinearities and current non-contact transducers are unable to create such amplitudes. To solve this problem, there is need for the development of a non-contact acoustic [2,3] source that is able to generate high amplitude signals.

This communication concerns a simulation study of a new concept, the “candy can” concept, recently developed and patented by a group at the Los Alamos National Laboratory (LANL, New Mexico, USA) that can be used for focused, high amplitude, non-contact excitation [4]. The “candy can” is a new type of non-contact ultrasonic transducer applying time reversal [5,6] to generate arbitrary signals with high amplitudes. The transducer consists of a number of piezo-transducers, located on the surface of a cavity. The concept thanks its name to a proof-of-concept prototype that used a crushed metallic candy can as a cavity.

Slide 1

Introduction Air-coupled time reversal

The “candy can”

A focused, high amplitude non-contact transducer

A new type of non-contact ultrasonic transducer able to generate **any arbitrary signal** in a sample with **amplitudes much higher** than those generated by conventional non-contact transducers.

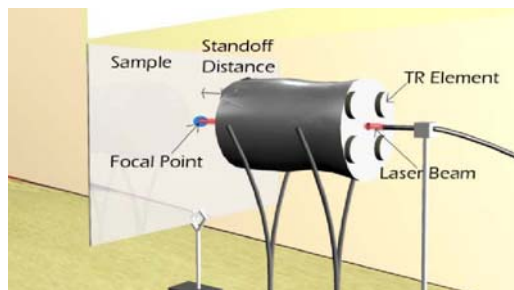


Figure: Proof-of-concept system developed at LANL.

XVII ICNEM

The non-contact source works as follows. The PZTs (TR elements) emit sound into a cavity one at a time. Sound leaks through a hole located near the sample and is detected by a laser on the sample surface. The laser vibrometer beam passes through the same hole that emits the sound. The detected signals are then time reversed and emitted simultaneously in phase from their respective piezo-transducers that are located on the cavity surface. The sound focuses on the sample surface at the laser point, creating an elastic wave source that propagates into the medium.

Slide 2

Introduction Air-coupled time reversal

Non-contact source applying time reversal

How does it work?

1. Emission of sound signals into cavity
2. Sound leaks through a hole located near the sample
3. Detection of sample surface response by laser
4. Time reversal of detected signals
5. Emission of time reversed signals
6. Focusing of sound on sample surface at laser point

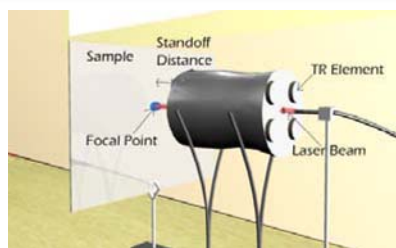


Figure: Proof-of-concept system developed at LANL.

XVII ICNEM

II. A SIMULATION STUDY

1. 2D Finite element model

To test and optimize the proposed concept, we implemented a 2D spectral finite element model in the commercial software package, Comsol Multiphysics [7,8]. The geometry of the model contains several domains, as can be seen in slide 3. A first domain corresponding to a cross section of a steel cavity in which the sound is emitted, a second domain corresponding to a rectangular aluminum plate on which the sound needs to be focused, a third and fourth domain corresponding to the air surrounding the cavity and the plate. At the top side of the cavity domain, a line was introduced corresponding to the transducer surface which is glued to the cavity. The computational region is surrounded by perfectly matching layers in order to suppress unwanted reflections from the edges.

Slide 3

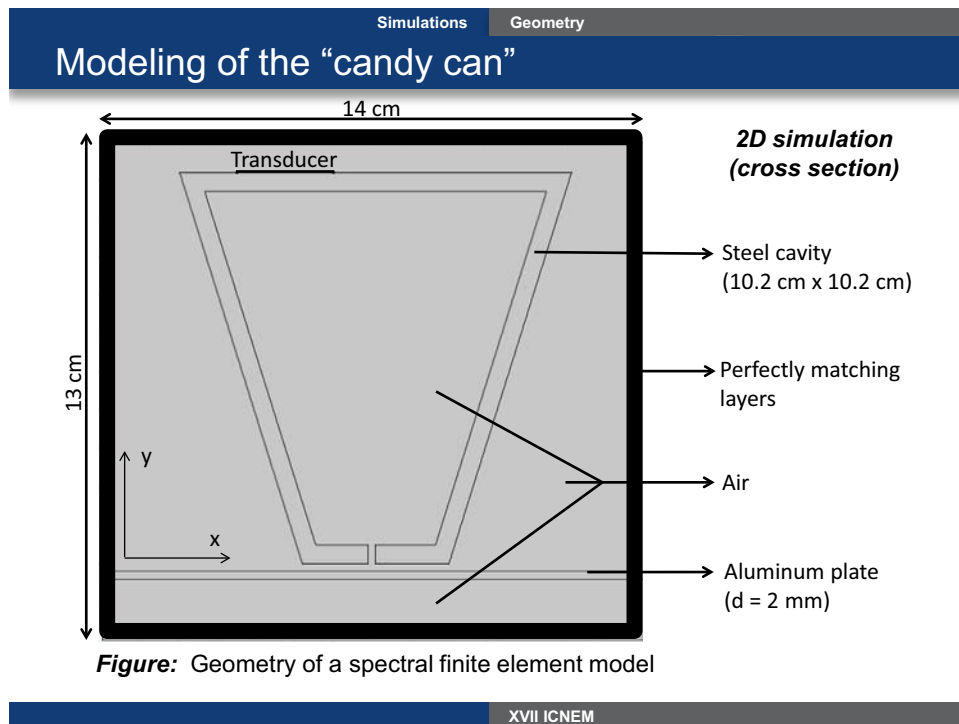
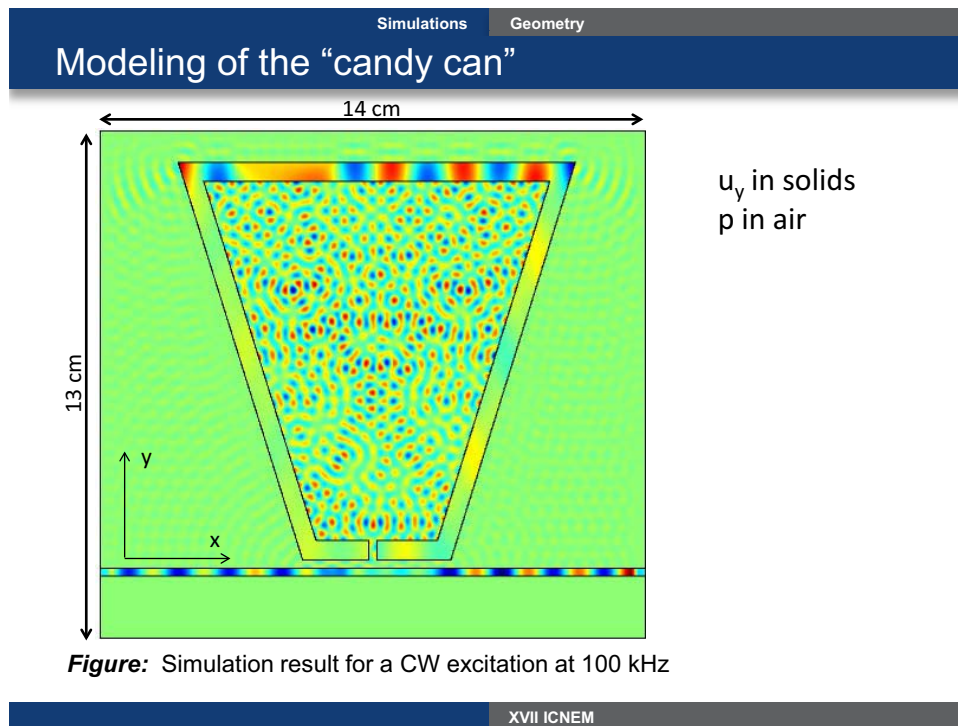


Figure: Geometry of a spectral finite element model

The model is finally solved for a number of frequencies. For instance, slide 4 shows the vertical displacement in the cavity shell and the aluminum plate and the pressure field in air for a continuous wave excitation at 100 kHz. One can clearly see that part of the excited sound wave is propagating through the cavity shell, while the rest is propagating into the air within the cavity. This part of the signal finally leaks through the cavity hole and reaches the aluminum plate, resulting in a wave propagating through the plate.

Slide 4



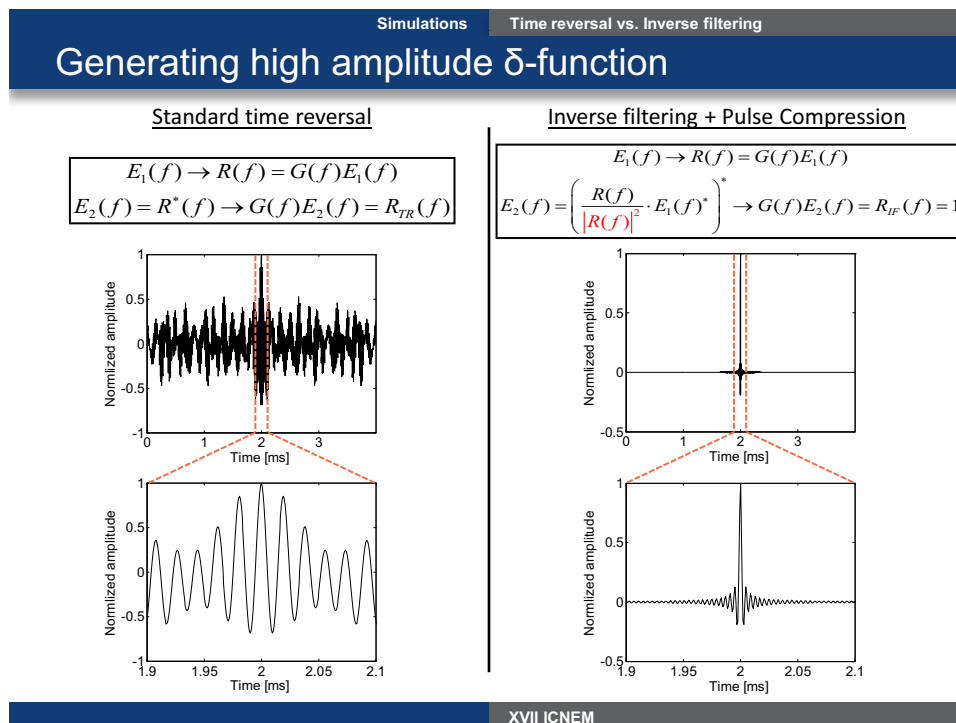
2. High amplitude excitation

In order to generate a high amplitude δ -function on the sample surface, two techniques were compared on slide 5. The first technique is the standard reciprocal time reversal technique [6]. In this technique a signal E_1 is first emitted by the receiver and a signal R is received at a position on the sample surface. In frequency domain, this signal corresponds to the product of the Green's function G with the emitted signal. The received signal is now reversed in time (in frequency domain this corresponds to taking the complex conjugate R^* of the signal) and re-emitted by the transducer. Finally, a high amplitude signal R_{TR} is received at the position on the plate surface where the first signal was recorded. The signal $R_{TR}(t)$ and a zoom of the signal around the focal time for a particular simulation are shown at the left hand side of slide 5. In this case, a considerable amount of noise is still observed around the focal peak.

To improve the quality of the focusing a second technique called inverse filtering [9] can be used in which the received signal R is not reversed in time directly, but only after convoluting the signal with the input signal and dividing it by the eigenmode energy. Re-emitting this signal by the receiver a nice δ -function is observed at the particular location on the sample surface. The received δ -function $R_{IF}(t)$ and a zoom of the function around the focal time are shown at the right hand side of slide 5.

If the received signal R is not only convoluted with the input signal, but also with an arbitrary signal D , the signal received at the sample surface will be the desired signal, as illustrated in slide 6. Doing this, any arbitrary signal can be focused on the sample surface.

Slide 5



Simulations Time reversal vs. Inverse filtering

Generating high amplitude arbitrary signal

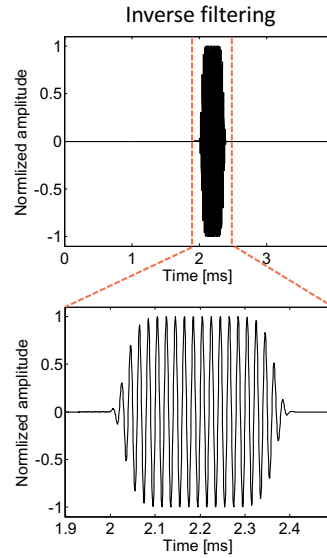
- If convolution is performed using
- 1) the inverse filtered signal
 - and
 - 2) an arbitrary signal D (e.g. burst)

$$E_1(f) \rightarrow G(f)E_1(f) = R(f)$$

$$E_2(f) = \left(\frac{R(f)}{|R(f)|^2} \cdot D(f)^* \cdot E_1(f)^* \right)^* \rightarrow G(f) \cdot E_2(f) = D(f)$$



The focusing signal will be the
desired signal

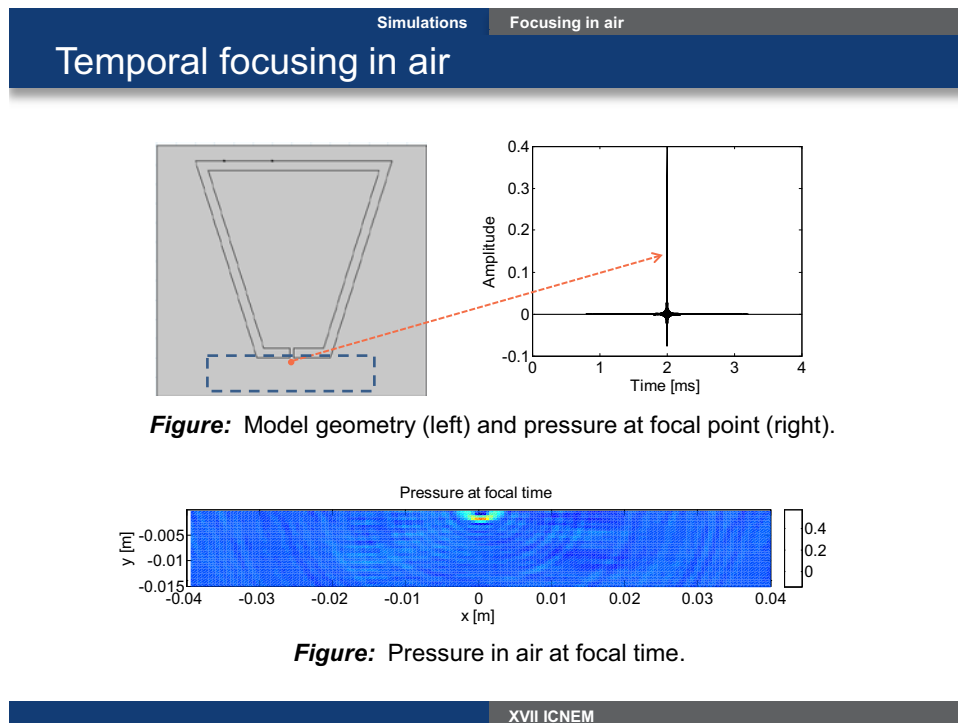


3. Simulation results

3.1. Focusing in air

To start with, we studied the possibility to focus energy in air using the new non-contact transducer. The top figures in slide 7 show the model geometry (left) and the pressure (right) measured at a particular location in air, i.e. $(x, y) = (0, -2)$ mm, underneath the cavity after inverse filtering. A clear focusing peak can be observed. The bottom figure shows a snapshot of the pressure field in air within a rectangle around the focal point (the rectangle is drawn in the model geometry top figure) at the focal time. In this figure, the spatial focal point is at the position where the direct signal was received.

Slide 7



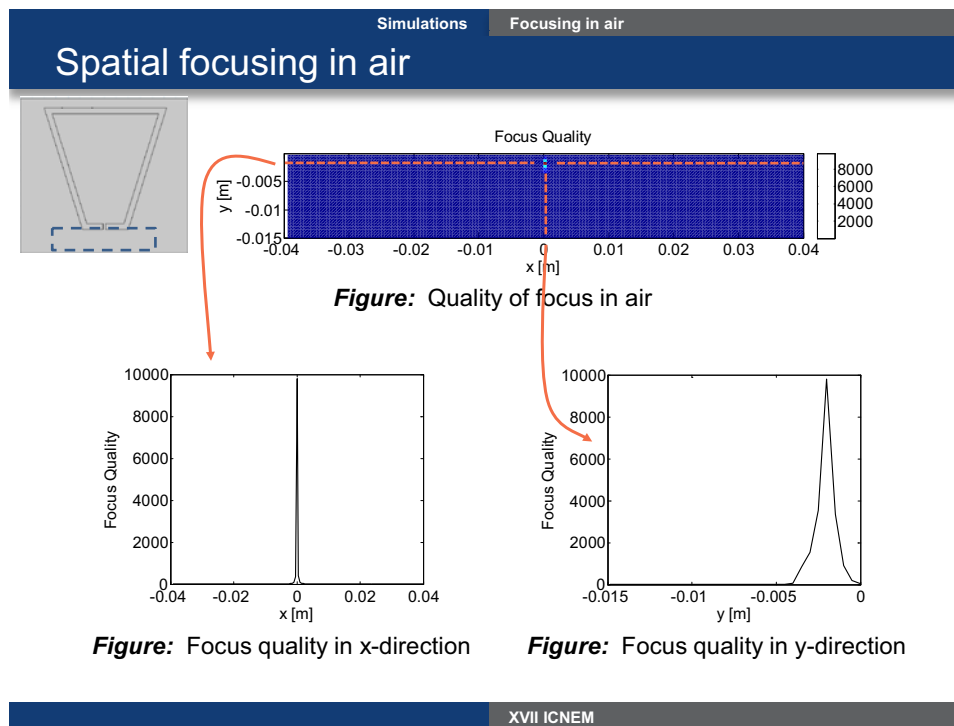
An even more clear view of the focal spot is obtained by calculating for every point in the computational domain the quality of the focus using the following formula:

$$Quality = \frac{\text{mean}_{t \in [t_{MAX} - \Delta t, t_{MAX} + \Delta t]} (R_{IF}(t)^2)}{\text{mean}_{t \notin [t_{MAX} - \Delta t, t_{MAX} + \Delta t]} (R_{IF}(t)^2)}$$

where t_{MAX} is the focal time and Δt a small time window. Hence, this quality formula calculates the mean energy around focal time and divides it by the mean of the energy elsewhere. In slide 8, the quality was calculated in every point within a rectangle around the focal spot. It is obvious that high quality values are observed at the position of the focal point, which is clearly observable in the bottom

plots of the quality in both x- and y-direction. The quality plot gives an idea of the spatial extent of the obtained focus.

Slide 8



3.2. Focusing on solid half space

Next, we used the non-contact transducer to focus energy on a solid aluminum half space. The top figures in slide 9 show the model geometry (left) and the displacement (right) measured at a particular location, i.e. $(x, y) = (0, -4)$ mm, on the surface of the half space after inverse filtering. Again, a clear focusing peak is observed. The spatial focal point at that position is observed when displaying the vertical displacements in a rectangular region at the focal time (bottom figure).

The quality of the focus can be calculated using the same formula as mentioned before. Again, high quality values are observed at the intended position (see slide 10).

Slide 9

Simulations Focusing on plate surface
Temporal focusing on solid half space

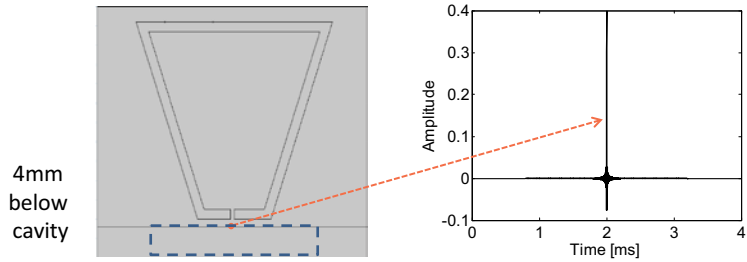


Figure: Model geometry (left) and vertical displacement at focal point (right).

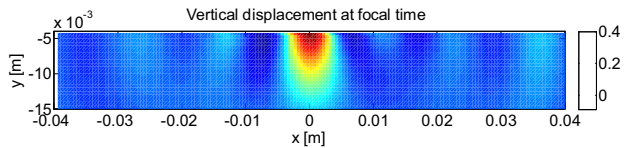


Figure: Vertical displacement in aluminum half space at focal time.

XVII ICNEM

Slide 10

Simulations Focusing on plate surface
Spatial focusing on solid half space

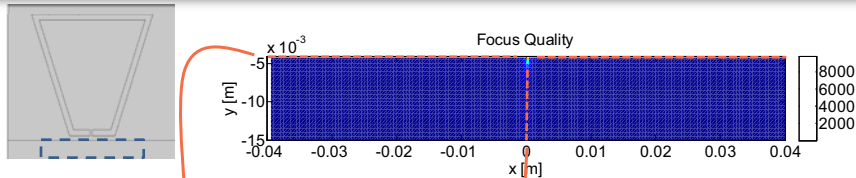


Figure: Quality of focus in the half space

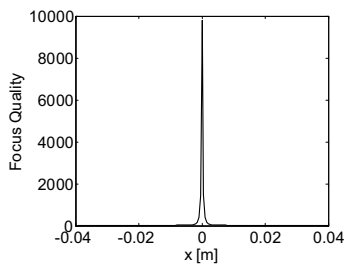


Figure: Focus quality in x-direction

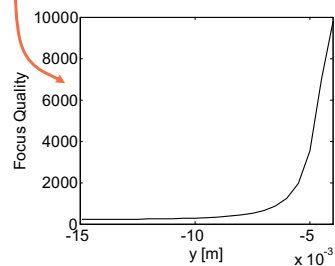
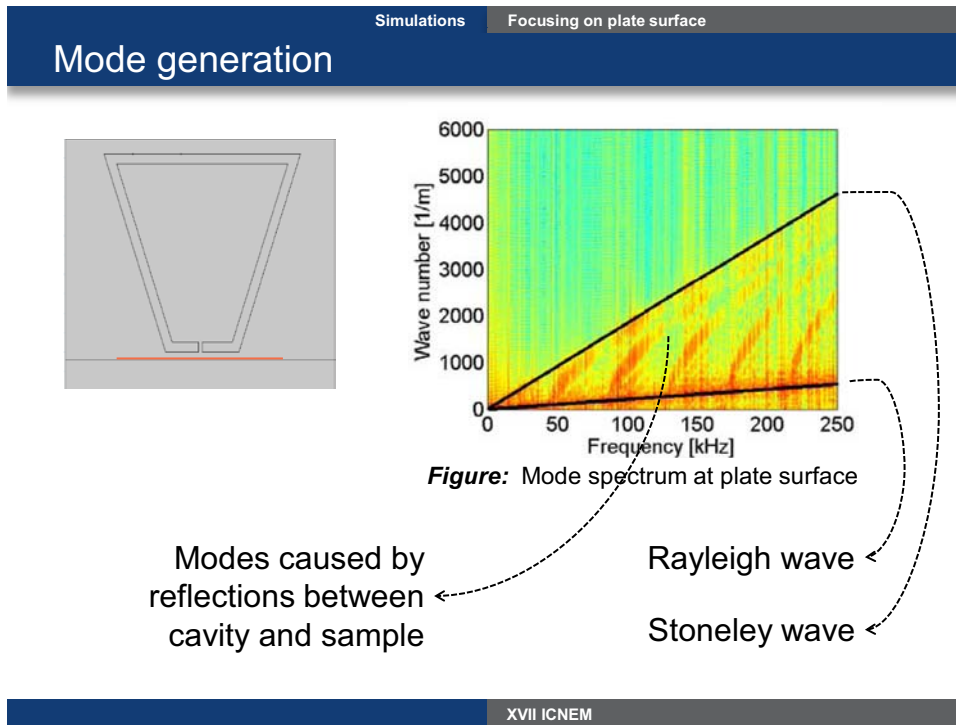


Figure: Focus quality in y-direction

XVII ICNEM

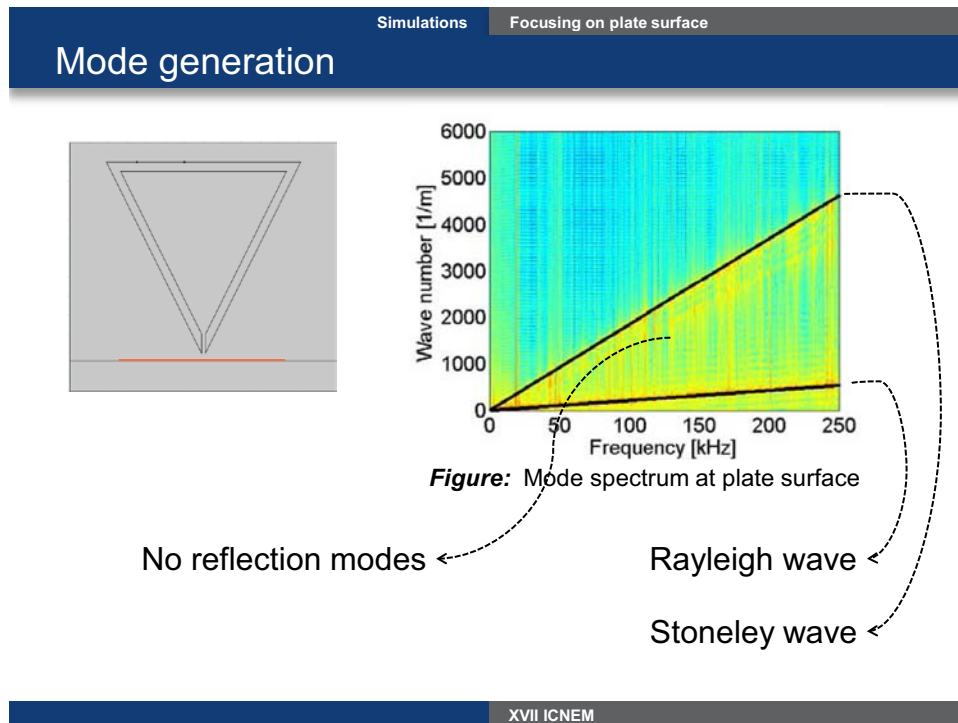
We already demonstrated the ability to focus sound at a particular location on the sample surface. This focusing, however, creates an elastic wave source that propagates into the medium. This can be illustrated by determining the different modes present in the sample after the sound has focused on the sample surface. Calculating the vertical displacements on a line along the surface of the sample (orange line in the left plot of slide 11) and taking a 2D Fourier transform of those signals we get the wave number-frequency plot shown at the right hand side, where different wave modes can be distinguished: two modes of waves propagating along the surface of the sample (Rayleigh and Stoneley wave) and a few modes caused by reflections between the sample and the cavity.

Slide 11



To demonstrate that most of the modes discussed in the previous slide were indeed caused by reflections between cavity and sample, we modeled another type of cavity with a sharp edge at the location of the hole. Due to the fact that none of the faces of the cavity is parallel to the sample, no reflections between cavity and sample will occur and only the Rayleigh wave and Stonley wave modes remain, as can be seen in the mode plot.

Slide 12



3.3. Focusing on small plate

Finally, we studied the ability to focus on a small aluminum plate. Again, the top figures in slide 13 show the model geometry (left) and the vertical displacement focusing signal (right) measured at a particular location on the surface of the plate, i.e. $(x, y) = (0, -4)$ mm. The bottom figure shows a snapshot of the vertical displacement at focal time, illustrating the spatial focal point.

The quality plot of the focus on slide 14 shows that in this case, the focal spot is not limited to a spot on the surface of the sample but spreads out over the entire thickness of the plate. This is also seen in the quality plots in x- and y-direction.

Slide 13

Simulations Focusing on plate surface
Temporal focusing on small plate ($d = 2\text{ mm}$)

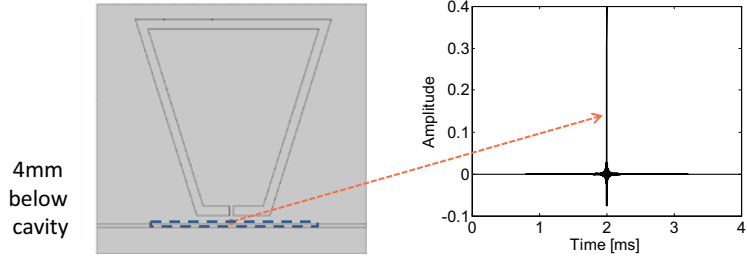


Figure: Model geometry (left) and vertical displacement at focal point (right).

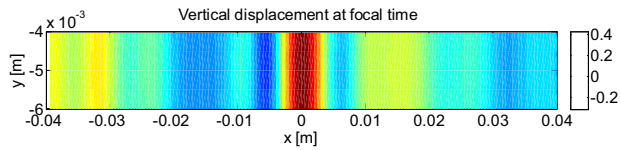


Figure: Vertical displacement in aluminum plate at focal time.

XVII ICNEM

Slide 14

Simulations Focusing on plate surface
Spatial focusing on small plate ($d = 2\text{ mm}$)

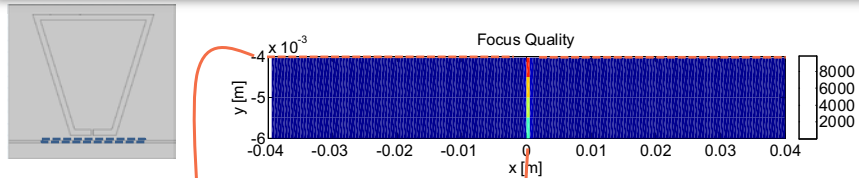


Figure: Quality of focus in the plate

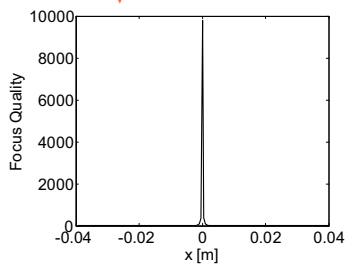


Figure: Focus quality in x-direction

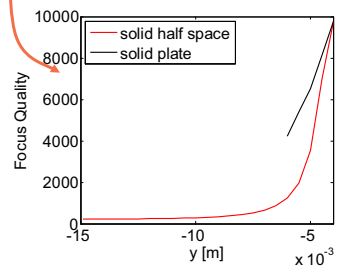
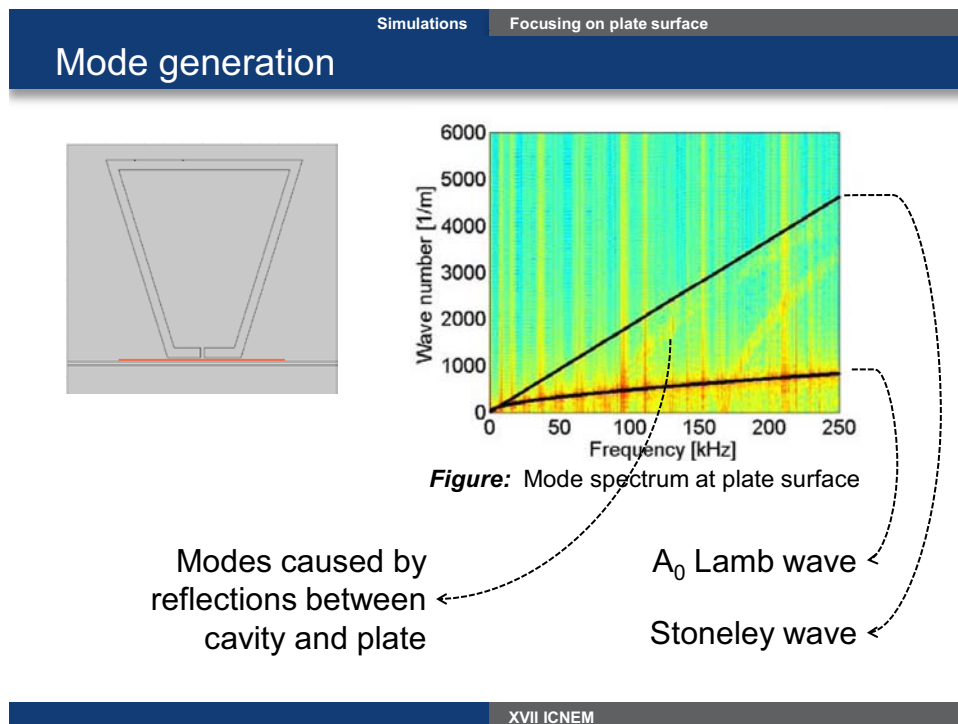


Figure: Focus quality in y-direction

XVII ICNEM

As in the case of the solid half space, the focused sound creates elastic waves propagating through the plate. Studying the wave number-frequency plot on slide 15, the modes occurring here are those of a surface propagating Stoneley wave, an A_0 Lamb wave propagating along the plate and extra modes caused by reflections between the cavity and the plate. These extra modes can be removed by using another type of cavity as discussed in the previous example.

Slide 15



In the previous simulations, we each time focused on a point on the sample surface right under the cavity hole. This, however, is not the only location where energy can be focused. This is illustrated on slide 16. The top figures show the model geometry (left) and the vertical displacement focusing signal (right) measured at a particular location on the surface of the plate, i.e. $(x, y) = (20, -4)$ mm, somewhere to the right of the cavity hole. As can be seen, we are also able to create a focus at that position. The bottom figure shows a snapshot of the vertical displacement at focal time, illustrating the spatial extent of the focus.

On slide 17, the quality plot for this focus is shown. High quality values are obtained at the position of the focal point.

Simulations Focusing on plate surface
Temporal focusing on small plate ($d = 2$ mm)

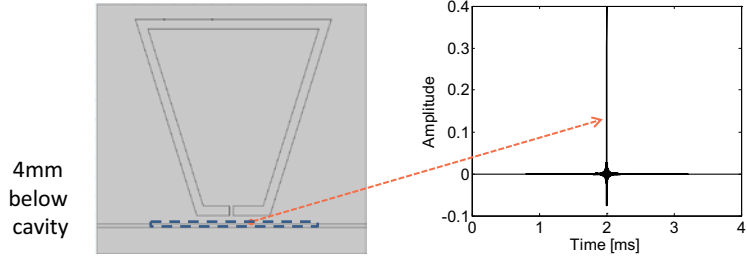


Figure: Model geometry (left) and vertical displacement at focal point (right).

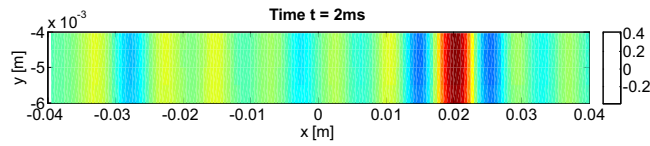


Figure: Vertical displacement in aluminum plate at focal time.

Simulations Focusing on plate surface
Spatial focusing on small plate ($d = 2$ mm)

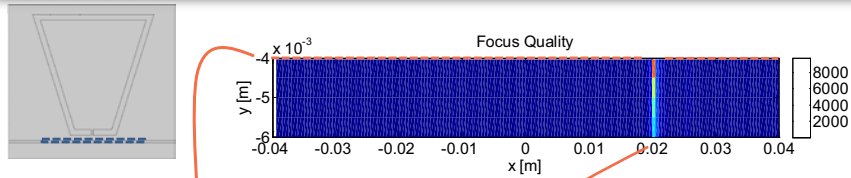


Figure: Quality of focus in the plate

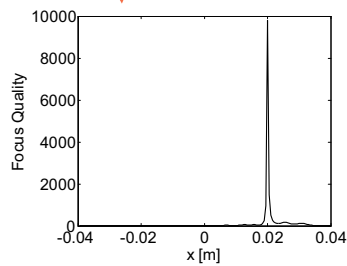


Figure: Focus quality in x-direction

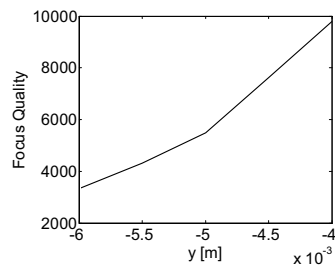


Figure: Focus quality in y-direction

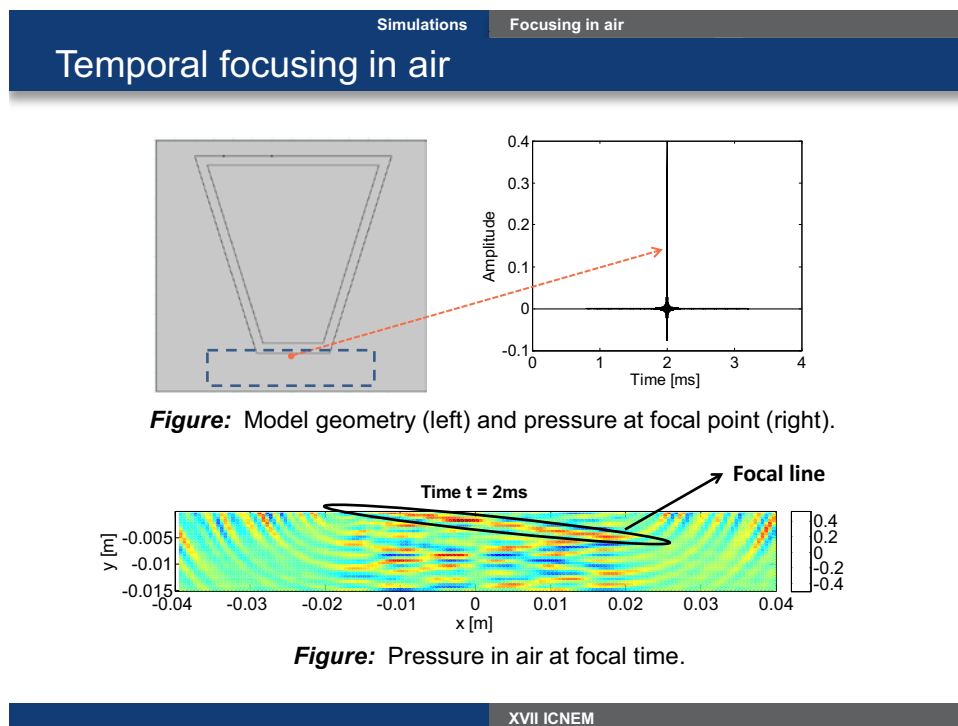
3.3. Focusing using a closed cavity

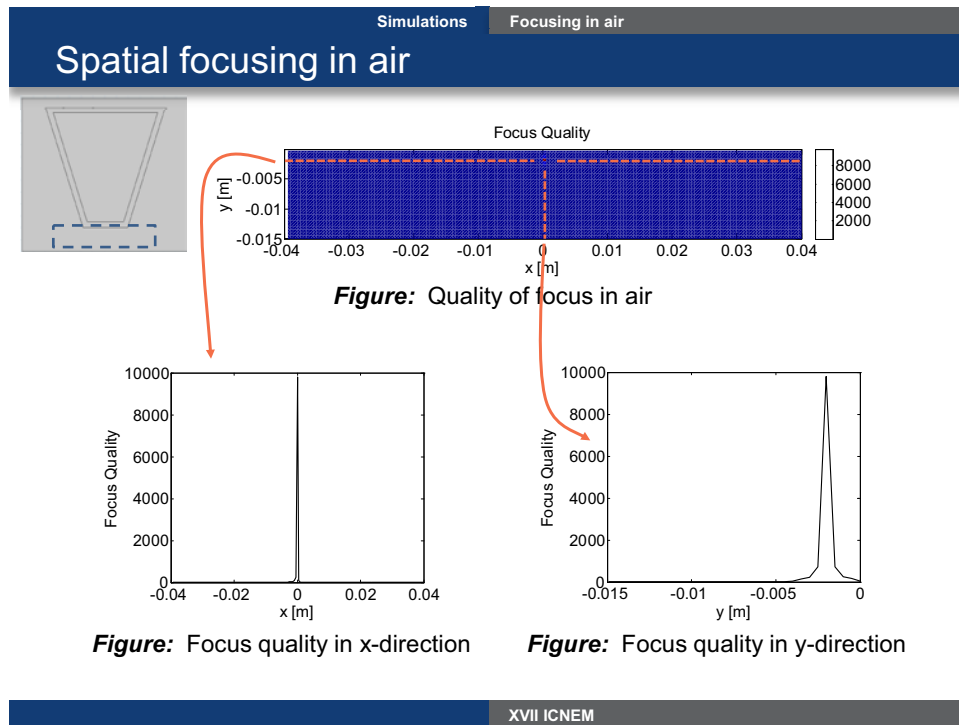
The previous results demonstrated the ability of the non-contact source to focus energy at any possible location in air or on a sample surface. However, we are now wondering if it is really needed to have a hole in the cavity through which sound leaks. We therefore constructed a cavity, similar to the one used in the previous simulations, but this time without a hole and we redid some of the previous simulations.

As a start, we studied the possibility to focus energy in air. On slide 18, the top figure shows the model geometry (left) and the pressure focusing signal (right) measured at the location $(x, y) = (0, -2)$ mm in air. A nice focal peak is observed in the time signal. However, in the bottom figure, where a snapshot of the pressure field at focal time is shown, it seems that we have a focal line rather than a focal spot. This can be explained by the fact that most of the energy that contributes to the focus is coming from the bottom edge of the cavity, resulting in a line of energy, while in the previous results most of the energy used to create the focus was energy coming from a small hole, resulting in a focal spot.

Studying the quality plot of the focus on slide 19, we notice that although the snapshot at focal time suggests a weaker focus, the quality of the focus is still good.

Slide 18





A similar simulation is now performed to focus on a small aluminum plate. The top figure in slide 20 shows the model geometry (left) and the focusing signal of the vertical displacement (right) measured at the location $(x, y) = (0, -4)$ mm at the plate surface. The bottom figure shows a snapshot of the vertical displacements in the plate at focal time. In this case, a nice focal spot at focal time can be observed in contrast to the previous results. Despite the fact that most of the energy that contributes to the focus again comes from the bottom edge of the cavity, we now have additional contributions from the plate itself, resulting in a better focus.

The quality plot of the focus is depicted in slide 21, showing high quality values at the location of the focus.

Slide 20

Simulations Focusing on plate surface
Temporal focusing on small plate ($d = 2\text{ mm}$)

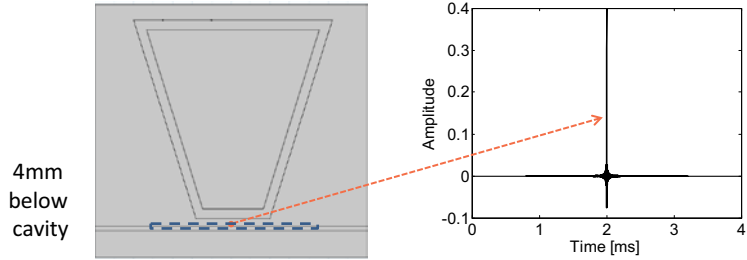


Figure: Model geometry (left) and vertical displacement at focal point (right).

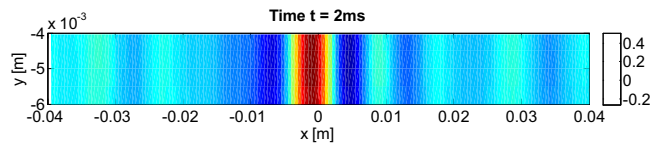


Figure: Vertical displacement in aluminum plate at focal time.

XVII ICNEM

Slide 21

Simulations Focusing on plate surface
Spatial focusing on small plate ($d = 2\text{ mm}$)

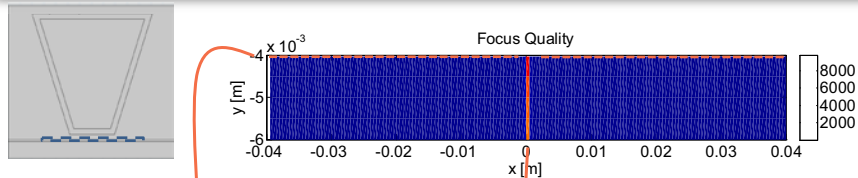


Figure: Quality of focus in the plate

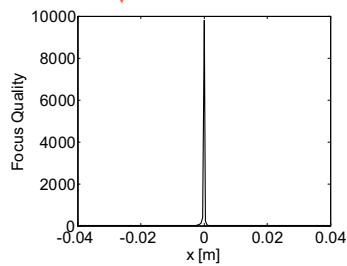


Figure: Focus quality in x-direction

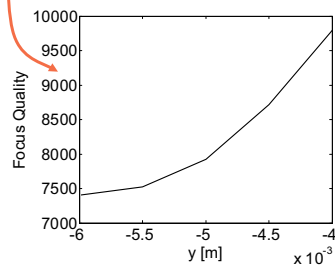


Figure: Focus quality in y-direction

XVII ICNEM

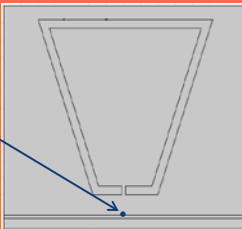
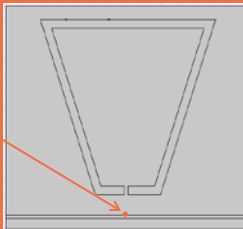
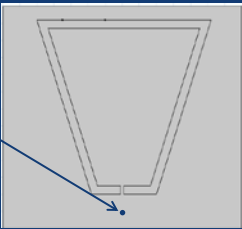
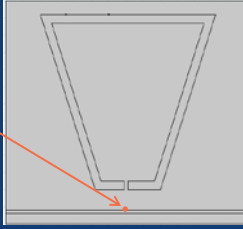
3.4. Transducer calibration

Let us now again study the cavity with a hole in the bottom surface. Until now, the time reversal procedure was done as follows (see orange part slide 22): we record a signal at a particular location on a sample (for instance on the surface of a small plate) and re-emit this signal in a time reversed way into the cavity in order to focus on the location of the recorded signal. This means that the transducer requires a calibration stage for each sample, signal and source position. Since this is very time consuming, certainly when you want to test different samples, we are wondering if we are able to remove the need for recalibration, by pre-calibrating the source in air and use those signals in the time reversal process (as illustrated in the blue part of the slide).

Slide 22

Simulations
Transducer calibration

Can we pre-calibrate transducer in air?

Step 2: Recording on plate	CONVENTIONAL	Step 5: Focusing on plate surface
		
Step 2: Recording in air	CALIBRATION	Step 5: Focusing on plate surface
		

XVII ICNEM

The calibration procedure will then work following the procedure discussed in slide 23. First a sound signal is emitted into the cavity and the pressure field in air is recorded. Then, a test sample is positioned (in the simulations 12 mm below the cavity) and a time reversed signal is re-emitted back into the cavity. This time reversed signal is calculated using the pressure signal measured in air at the exact same location of the surface of the test sample. Finally, sound should focus on the surface of the sample.

Slide 23

Simulations Transducer calibration

Can we calibrate transducer in air?

Calibration procedure

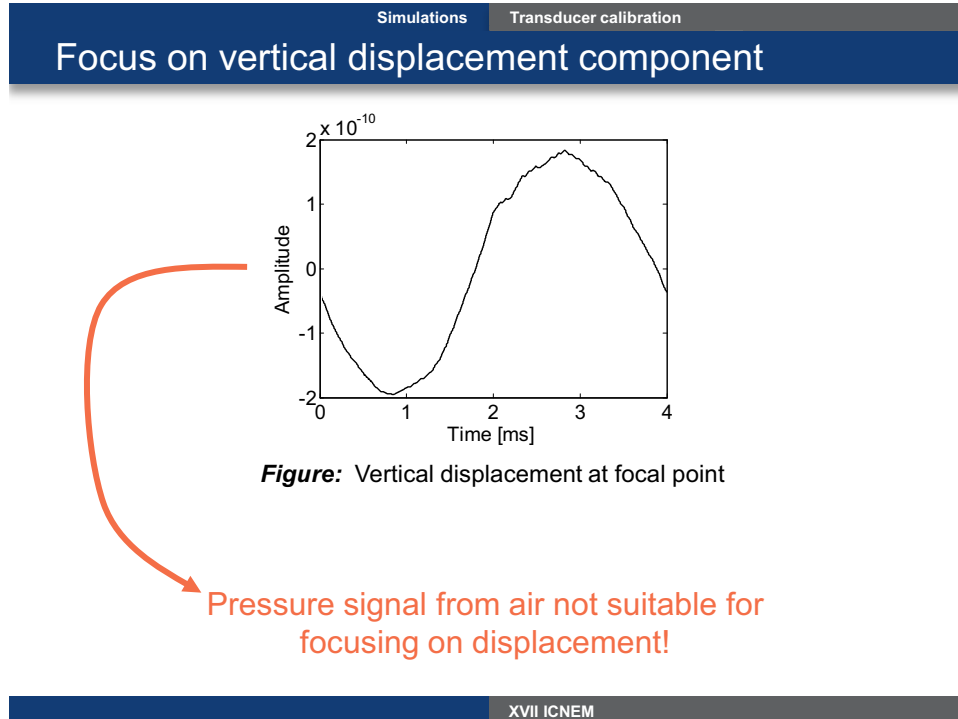
1. Emission of sound into cavity
2. Measuring pressure in air
3. Positioning of test sample
4. Emission of time reversed / inverse filtered signal
5. Focusing of sound on sample surface

12 mm below cavity

XVII ICNEM

We first studied the ability to focus the vertical displacement component on the plate surface using the recorded pressure signals in air. In slide 24, the vertical displacement focusing signal at the plate surface is plotted. It is obvious that the calibration method is not working in this case.

Slide 24



Studying the normal stress component on the plate surface however (slide 25), we see a nice focusing peak at the focal point, next to a few subsequent focus moments due to reflections between plate and cavity. The bottom figure shows a snapshot of the normal stress at focal time, illustrating the focal spot at the sample surface.

The quality plot of the focus (slide 26) also shows a nice focal spot at the intended location.

Slide 25

Simulations Transducer calibration
Focus on normal stress component

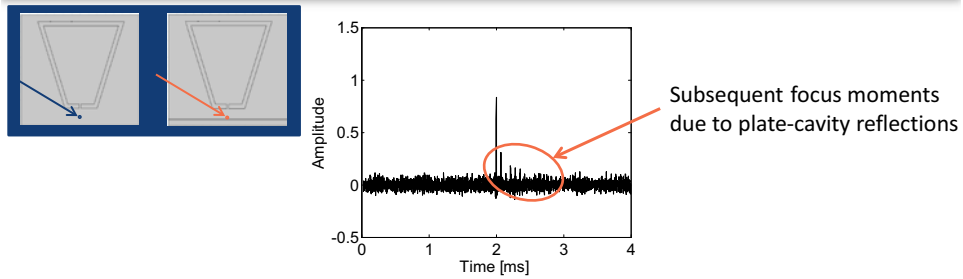


Figure: Normal stress at focal point

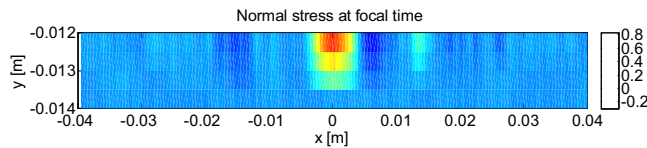


Figure: Normal stress in aluminum plate at focal time.

XVII ICNEM

Slide 26

Simulations Transducer calibration
Focus on normal stress component

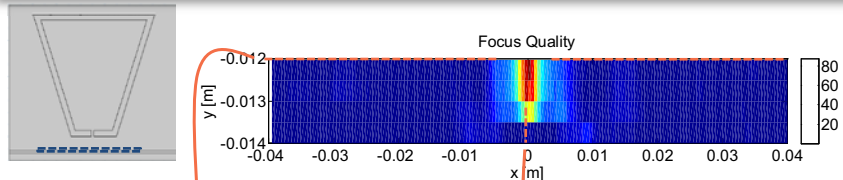


Figure: Quality of focus in the plate

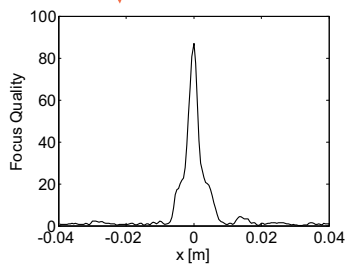


Figure: Focus quality in x-direction

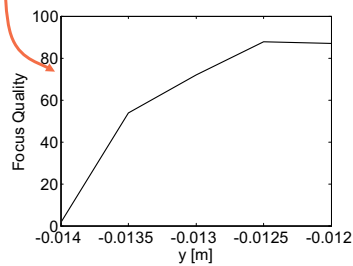
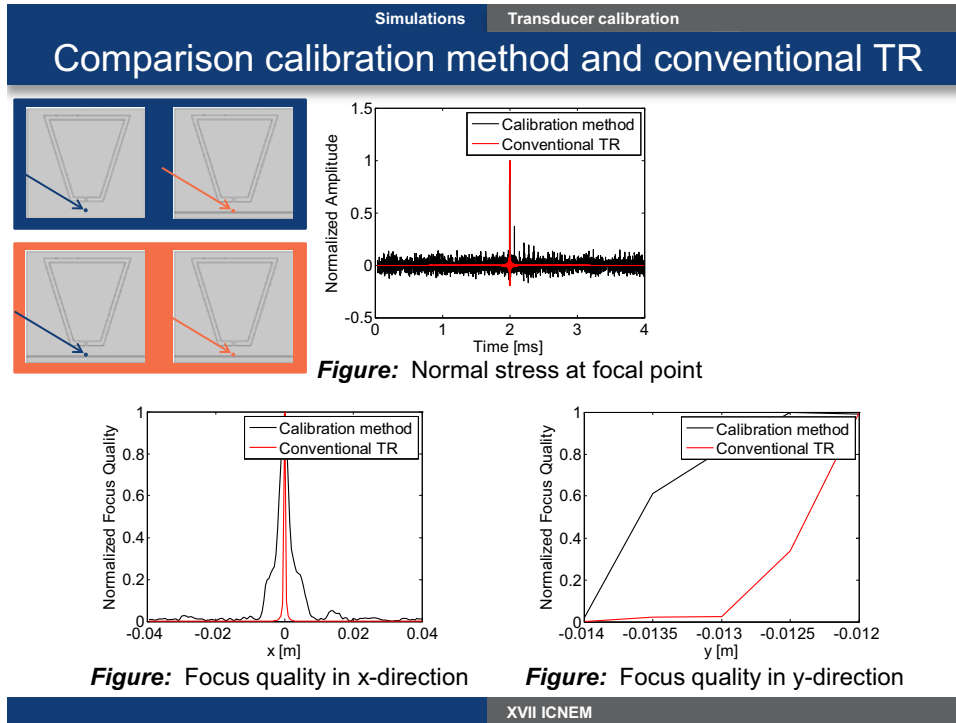


Figure: Focus quality in y-direction

XVII ICNEM

In slide 27 the results of the conventional TR method (illustrated in the orange box) are compared with the results of the calibration method (illustrated in the blue box). Although the focus quality is a bit less when using the calibration method, i.e. focal spot has a larger spatial extent, the calibration method gives still satisfying results compared to the conventional method.

Slide 27



On slide 28, we studied the possibility to use the calibration method in case of a closed cavity. The top figure shows the focusing signal at the focal point. The bottom figure shows the quality plot obtained with this set-up. It is obvious that in both figures no clear evidence of a focus is found. This is probably due to the fact that the focusing in air did not perform that good using a closed cavity (see slide 18 where we had a focal line instead of a focal spot). Since the signals in air are used as reference signals in the calibration, it is obvious that the focusing will not work in this case either.

Slide 28

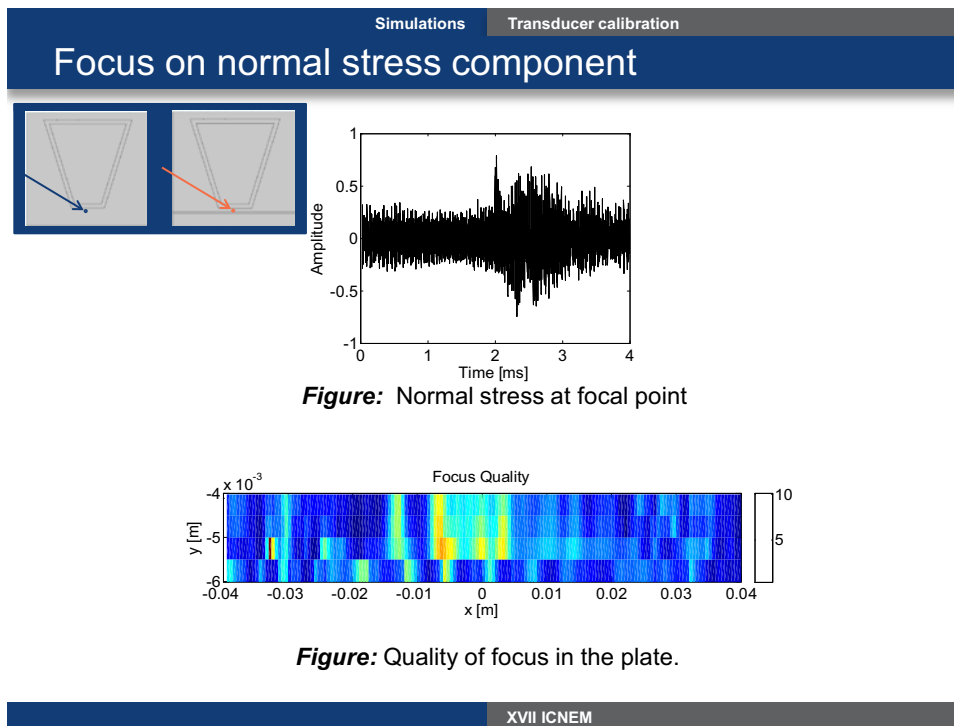
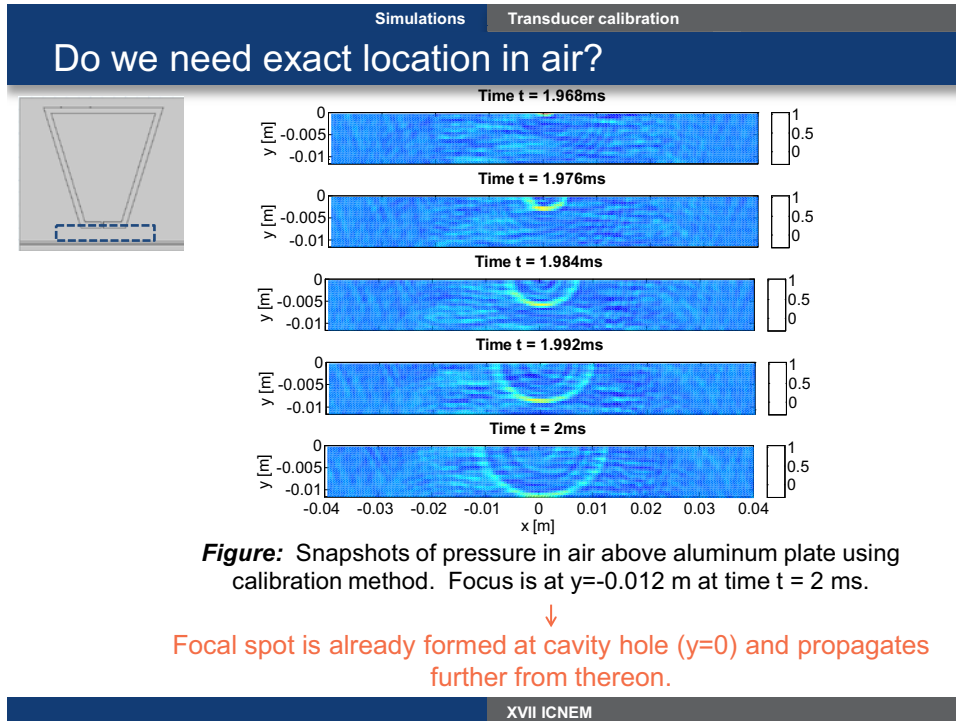


Figure: Normal stress at focal point

Figure: Quality of focus in the plate.

The previous results showed that the calibration method works well in case of a cavity with hole if we rebroadcast the pressure signal recorded at the exact same location of the surface of the sample that is placed afterwards below the cavity. We are now wondering if this is really needed. Can we also use pressure signals lying closer to the cavity than the sample surface? The figure in slide 29 illustrates what exactly happens in the air above the sample after the pressure signal is re-emitted into the cavity. To create a focus on the sample surface, the focal spot already forms at the cavity hole and then propagates further in air from thereon. This means that it should also be possible to focus sound on the sample surface using a pressure signal measured at a location somewhere closer to the cavity.

Slide 29



This is illustrated in slide 30. We measured the pressure at different locations in air (respectively at -12 mm, -9 mm, -6 mm, -3 mm and 0 mm). Those signals were then used to focus on the normal stress on the surface of a plate positioned 12 mm below the cavity ($y=-12$ mm). At the left hand side of the slide you can see the different measured focusing signals and a zoom of the signals. As can be seen, each situation results in a focusing, however the amplitude of the focusing diminishes as the pressure signal was recorded closer to the cavity due to absorption in air.

Studying the quality of the focus (slide 31), one can see that the spatial extent of the focal spot is approximately the same in each situation.

Simulations Transducer calibration

Do we need exact location in air?

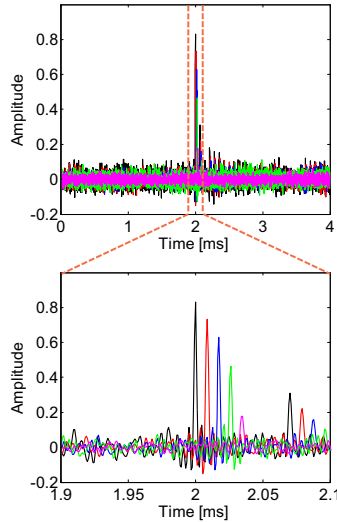
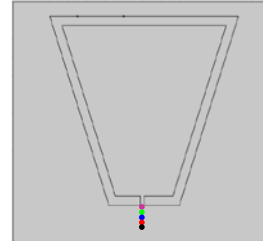


Figure: Normal stress at plate surface

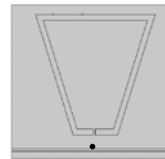
Pressure measurement locations:

- y = -12 mm
- y = -9 mm
- y = -6 mm
- y = -3 mm
- y = 0 mm



Position top surface plate:

- y = -12 mm



Simulations Transducer calibration

Do we need exact location in air?

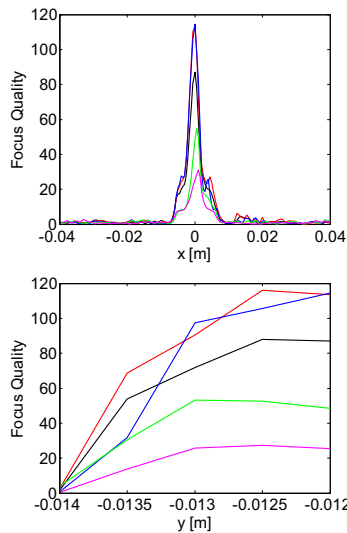
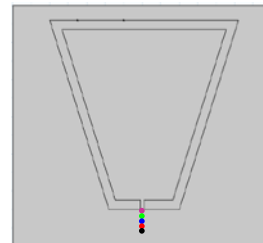


Figure: Focus quality in x- and y-direction

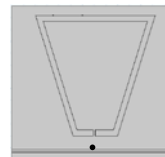
Pressure measurement locations:

- y = -12 mm
- y = -9 mm
- y = -6 mm
- y = -3 mm
- y = 0 mm



Position top surface plate:

- y = -12 mm



III. Conclusion & future plans

Slide 32

Simulations
Conclusion

Conclusion & Future plans

Conclusion

- FEM model of the “candy can” concept was developed
- Principle of high amplitude non-contact excitation was illustrated
- Focusing quality can be improved by using inverse filtering
- “Candy can” can be pre-calibrated in air

Future plans

Parametric study to determine influence of:

- cavity material and shape
- cavity and hole dimensions
- position of transducers
- ...

XVII ICNEM

IV. References

- [1] Guyer, R., and Johnson P. *Nonlinear Mesoscopic Elasticity: The complex behavior of granular media including rocks and soil*. Wiley-VCH, 2009.
- [2] Solodov, I., Pfleiderer, K., Gerhard, S., Predak, S. and Busse, G. New opportunities for NDE with air-coupled ultrasound. *NDT&E Int.* 39 (2006), 176-183.
- [3] Solodov, I., Stoessel, R. and Busse, G. Material characterization and NDE using focused slanted transmission mode of air-coupled ultrasound. *Res. Nondestruct. Eval.* 15 (2004), 65-85.
- [4] Ulrich, T.J., Anderson, B. and Le Bas, P.Y. *Time Reversal Acoustic Noncontact Source*. US Patent 2011/0247419 A1 (2011).
- [5] Fink, M. Time reversed acoustics. *Phys. Today* 50 (1997), 34-40.
- [6] Anderson, B., Griffa, M., Larmat, C., Ulrich, T.J. and Johnson, P. Time reversal. *Acoustics Today* 4 (2008), 5-16.
- [7] COMSOL Multiphysics User's Guide, Version 4.2a (2011).
- [8] COMSOL Multiphysics Acoustics Module User's Guide, Version 4.2a (2011).
- [9] Tanter, M., Thomas, J. and Fink, M. Time reversal and the inverse filter. *J. Acoust. Soc. Am.* 108 (2000), 223-234.